

First-principles study of strain stabilization of Ge(105) facet on Si(001)

Guang-Hong Lu,^{1,2} Martin Cuma,³ and Feng Liu^{2,*}

¹*School of Science, Beijing University of Aeronautics and Astronautics, Beijing 100083, China*

²*Department of Materials Science and Engineering, University of Utah, Salt Lake City, Utah 84112, USA*

³*Center for High Performance Computing, University of Utah, Salt Lake City, Utah 84112, USA*

(Received 27 May 2005; published 9 September 2005)

Using the first-principles total energy method, we calculate surface energies, surface stresses, and their strain dependence of the Ge-covered Si (001) and (105) surfaces. The surface energy of the Si(105) surface is shown to be higher than that of Si(001), but it can be reduced by the Ge deposition, and becomes almost degenerate with that of the Ge/Si(001) surface for three-monolayer Ge coverage (the wetting layer), leading to the formation of the {105}-faceted Ge hut. The unstrained Si and Ge (105) surfaces are unstable due to the large tensile surface stress originated from the surface reconstruction, but they can be largely stabilized by applying an external compressive strain, such as by the deposition of Ge on Si(105). Our study provides a quantitative understanding of the strain stabilization of Ge/Si(105) surface, and hence the formation of the {105}-faceted Ge huts on Si(001).

DOI: [10.1103/PhysRevB.72.125415](https://doi.org/10.1103/PhysRevB.72.125415)

PACS number(s): 68.35.Md, 61.46.+w, 68.35.Bs, 68.35.Gy

I. INTRODUCTION

Heteroepitaxial growth of strained thin films proceeds generally via the Stranski-Krastanov (SK) growth mode,¹ characterized by layer-by-layer growth, followed by formation of three-dimensional (3D) islands. The 3D islands may form with crystalline perfection and remain coherent with the substrate (free of dislocations).^{2,3} For semiconductor films with high surface energy anisotropy, the islands are bounded by specific “low-energy” facets. A prototype model system of the SK growth is the formation of faceted Ge islands (huts) on the Si(001) substrate,³ characterizing the 2D-to-3D growth transition.

Thermodynamic balance between surface/interface energies controls the equilibrium growth mode (layer-by-layer versus island formation).¹ Qualitatively, it is well understood that the formation of strained 3D islands is driven by relaxation of the strain energy at the expense of the increase of the surface energy. Strain energy increases with increasing film thickness. The relaxation of the strain energy via 3D island formation scales with island volume, while cost of surface energy scales with island surface area. Thus, beyond a critical thickness, relaxation of the strain energy will overcome the cost of the surface energy for a sufficiently large island, leading to island formation.

Understanding the SK growth of the strained island formation requires knowledge of surface energies and their strain dependence of both the wetting layer and island surfaces. Despite extensive studies that have been carried out so far,⁴⁻⁷ our understanding is still limited at a qualitative level. This is partly because quantitative information of island surface energies for most systems is unknown. In principle, island surface energies can be determined from first-principles calculations. However, facets on strained 3D islands are generally high-index surfaces, which involve complex reconstructions that are difficult to determine. For example, the Ge hut on Si(001) is bounded by {105} facets,³ but it is not until recently that the correct surface reconstruction of the strained Ge(105) surface has been finally determined⁸⁻¹⁰ in accor-

dance with an original suggestion by Khor and Sarma.¹¹ On the other hand, surface energies of the Ge/Si(001) surface (wetting layer surface) have been calculated either by using a less-accurate empirical potential¹² or first-principles potential but only for relative energies.¹³ The absolute surface energies and their strain dependence, however, have not been completely determined from first principles.

Furthermore, the surface stresses of both the wetting layer and the island surfaces are also very important to the understanding of strained island formation. A facet on a strained island forms often due to strain stabilization, while its original structure is not stable without applying the external strain. For example, the strained Ge(105) facets on the hut are stable, but Si(105) and Ge(105) facets are unstable at their respective equilibrium lattice constant. Scanning tunneling microscopy (STM) studies have shown that the clean Si(105) surface is always very rough and its roughness continues to decrease with increasing Ge deposition.^{8,9,14} This suggests that the (105) surface of Si is unstable and it is gradually stabilized by the increasing amount of compressive strain applied by Ge deposition. The strain stabilization of a surface structure is expected to correlate with its intrinsic surface stress. It has been speculated^{8,9,14} that there exists a large tensile stress in the Si(105) surface, rendering its instability. However, quantitative information of surface stress evolution in the Ge/Si(105) surface with increasing Ge coverage remains unknown, which causes a big gap in our understanding.

In this paper, we perform extensive first-principles supercell slab calculations to determine quantitatively surface energies, surface stresses, and their strain dependence of both Ge-covered Si(001) and (105) surfaces. Our calculations provide a quantitative understanding of the strain stabilization of the Ge(105) facet in comparison with the Ge(001) surface, and hence, the formation of the {105}-faceted Ge hut island on the Si(001) surface. Part of the results has been used as input parameters in a continuum model to quantitatively predict the critical size of hut nucleation and to assess the hut stability against coarsening.¹⁵

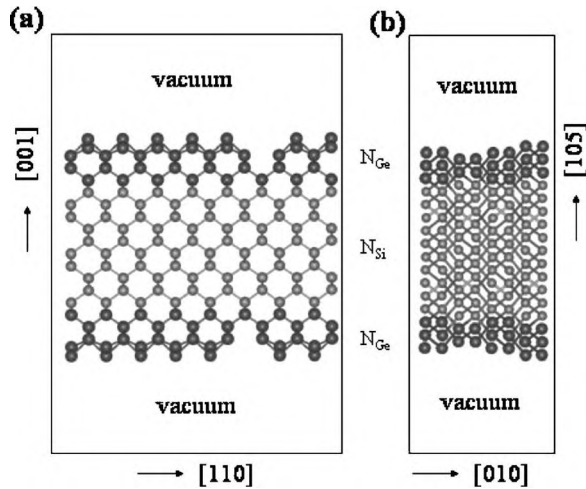


FIG. 1. Side view of the supercells of (a) Ge/Si(001)-(2×8) surface and (b) Ge/Si(105)-(2×1) surface used in the calculation (unrelaxed). N_{Si} and N_{Ge} represent the number of Si layers (light-gray spheres) and added Ge layers (dark-gray spheres), respectively.

II. METHODOLOGY AND COMPUTATIONAL DETAILS

We employ the plane-wave total-energy method based on the density functional theory and the local density approximation using the Vienna *Ab initio* Simulation Program (VASP).^{16,17} The ultrasoft pseudopotentials are used for both Si and Ge, and the plane-wave cutoff energy is 12 Ry. We use the $(2 \times N)$ -dimer-vacancy-line (DVL) reconstruction for the Ge-covered Si(001) surface,⁴ and the (2×1) -rebonded-step (RS) reconstruction for both the clean and Ge-covered Si(105) surface,^{8–10} as shown respectively in Fig. 1, and the $p(2 \times 2)$ reconstruction for the clean Si(001) surface. The supercells of the Ge/Si(001) and (105) surface are sampled by a (4×1) and (1×1) special k -point grid, respectively. The same reconstructions are used at both the top and bottom surfaces of the slab. We use ten (001)-layers of Si for the clean Si(001) surface, and 21 (105)-layers for the clean Si(105) surface, on which the Ge overlayers are added up to six (001)-layers and ~ 13 (105)-layers on both sides. The Si lattice is fixed at the calculated lattice constant of 5.40 Å, and the Ge layers are laterally strained by 4.3% according to the calculated lattice constant of 5.64 Å. The thickness of the vacuum layer is kept at 10 Å for all cases. All the atoms are fully relaxed until the forces on them are smaller than 10^{-3} eV/Å.

We accurately determine the bulk atom energies by calculating the total energy (E_T) as a function of the number of atoms (N) in the slab as¹⁸

$$E_T = 2AE_S + NE_B, \quad (1)$$

where A is the surface cell area and E_S and E_B denote the surface energy and the bulk atom energy, respectively. This assures the convergence of the surface energy with increasing Ge layers so that the Ge coverage dependence of the surface energy can be correctly assessed. The surface energies of Ge-covered Si surfaces are therefore calculated as

$$E_S = (E_T - N_{Si}E_B^{Si} - N_{Ge}E_{SB}^{Ge})/2A, \quad (2)$$

where N_{Si} and N_{Ge} are, respectively, the number of Si and Ge atoms in the slab and E_B^{Si} and E_{SB}^{Ge} are, respectively, the bulk atom energies of Si and strained Ge determined from Eq. (1).

To determine the surface stress tensors, we first calculate the bulk stress tensors of the slab supercell. The in-plane surface stress tensor σ_{ij}^s (rank-1) can then be simply calculated as^{12,19}

$$\sigma_{ij}^s = \frac{1}{2}c\sigma_{ij}, \quad (3)$$

where c is the lattice constant of the supercell in the surface normal direction. Factor 1/2 is added due to the presence of two equivalent surfaces. The indices i, j label the directions in the surface plane.

III. RESULTS AND DISCUSSION

To understand strain stabilization of the {105}-faceted Ge hut on Si(001) surface, we have calculated the surface energies and the surface stresses of both Ge/Si(001) and (105) surfaces as a function of Ge coverage and of pure Ge (001) and (105) surfaces as a function of strain.

A. Surface energy and surface stress of Ge-covered Si(105) and (001) surfaces

First, we briefly summarize surface energies of the clean Si(105) and Ge(105) surfaces. The surface energy of the Ge (105) surface is calculated to be 66.0 meV/Å², much lower than that of the Si(105) surface (94.2 meV/Å²). There are eight dangling bonds per unit cell in the (2×1) -RS Si and Ge (105) surface.^{8–10} Consequently, the surface energy of Ge(105) is lower than that of Si(105) because the dangling bond energy of Ge is lower.

Next, we demonstrate quantitatively how the strain stabilizes the Ge/Si(105) and Ge/Si(001) surfaces by calculating the surface energy of Ge-covered Si(105) and (001) surfaces as a function of Ge coverage. The results are shown in Fig. 2.

The surface energy of the Ge-covered Si(105) surface decreases continuously with increasing Ge coverage from the initial value of 94.2 meV/Å² of the clean Si(105) surface, and converges at ~ 11 layers of Ge to the final value of 61.4 meV/Å² of the Ge-covered Si(105) [We define here one Ge(105) layer thickness as $(\sqrt{26}/52)a_0$ (the label of upper x -axis in Fig. 2)]. The reduction of surface energy is largely achieved within the first 4–5 layers of Ge deposition. The continuous decrease of the surface energy of the Ge-covered Si(105) surface with increasing Ge coverage indicates that the clean Si(105) surface is unstable, but can be stabilized by the deposition of Ge layers. This is consistent with the experimental observation that a clean Si(105) surface has a very rough surface morphology^{8,9,14} but becomes smooth gradually with increasing Ge deposition.^{8,9}

In order to make a comparison between the (105) and (001) surfaces, we normalize the number of Ge(105)-layer (or thickness) to that of corresponding (001)-layer according to the fact that the (001) interplane spacing is about 2.55 times of that of (105). We use only the normalized layer

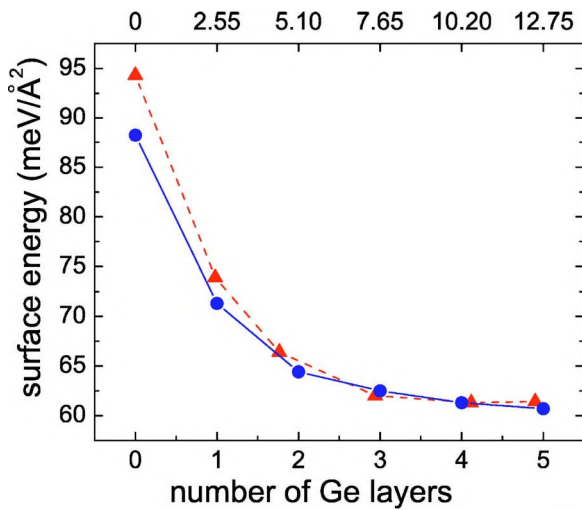


FIG. 2. (Color online) Surface energies of the Ge/Si(105) and (001) surfaces as a function of Ge coverage. Circles (solid line) and triangles (dashed line) represent, respectively, the Ge/Si(001) and (105) surface case. The upper x axis is labeled with the actual Ge(105) layers; the lower x axis is labeled with the actual Ge(001) layers or the normalized Ge(105) layers.

number of approximately 1, 2, 3, 4, and 5 (001)-layer(s), as shown in Fig. 2 (the label of lower x axis).

For the Ge-covered Si(001) surface, we obtain the surface energies with optimal N values for each coverage, i.e., $N = 10$ for one layer of Ge and $N = 8$ for higher coverage, which is consistent with both the experiments^{4,20} and the previous calculation.^{12,13} In comparison with the Si(105) surface (Fig. 2), the surface energy of the Si(001)- $p(2 \times 2)$ surface is much lower ($87.1 \text{ meV}/\text{\AA}^2$). Ge deposition reduces the surface energy of both surfaces, but the energy of the Ge/Si(105) surface decreases faster than that of Ge/Si(001). This results in the surface energy degeneracy of the two surfaces at about three monolayers of Ge coverage, and thus leads to the {105} facet formation on the Ge huts.

In order to quantify the amount of surface stress reduction of the Si(105) surface by the Ge deposition and, hence, to confirm the mechanism of strain stabilization of the Ge-covered Si(105) surface, we calculate the surface stress tensors of both the Ge/Si(105) and (001) surfaces as a function of the Ge coverage, as shown in Figs. 3(a) and 3(b). We define here a positive stress tensor as tensile stress, while a negative stress tensor as compressive stress. The average surface stresses, i.e., $(\sigma_{xx} + \sigma_{yy})/2$, of both the Ge/Si(001) and (105) surfaces are shown in Fig. 3(c).

The surface stress of the clean Si(105) surface are found to be tensile as large as $+192.3 \text{ meV}/\text{\AA}^2$ ($+179.7 \text{ meV}/\text{\AA}^2$ in the [010] direction and $+205.0 \text{ meV}/\text{\AA}^2$ in the $[\bar{5}01]$ direction, respectively), much larger than that of the clean Si(001) surface [$p(2 \times 2)$, $+81.1 \text{ meV}/\text{\AA}^2$], rendering its instability (Fig. 3). Our calculations further show that the large tensile stress in the Si(105) surface is originated from the (2×1) -RS surface reconstruction. The average surface stress of bulk-terminated Si(105)- (1×1) surface is only $+84.2 \text{ meV}/\text{\AA}^2$ in both the [010] and $[\bar{5}01]$ directions. Thus, the reconstruction lowers the Si(105) surface energy from

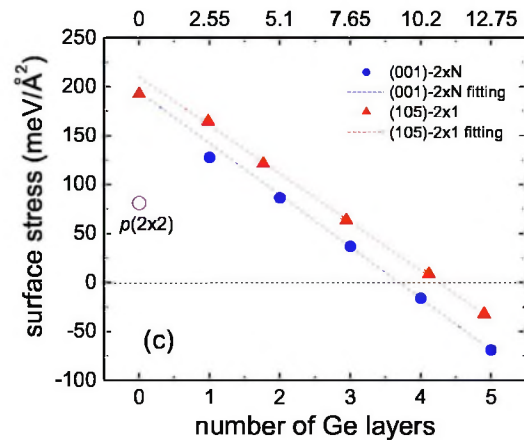
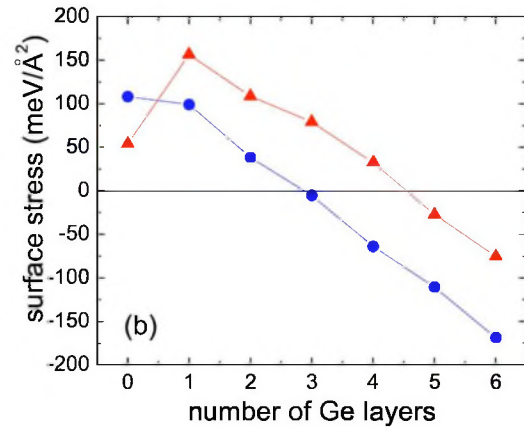
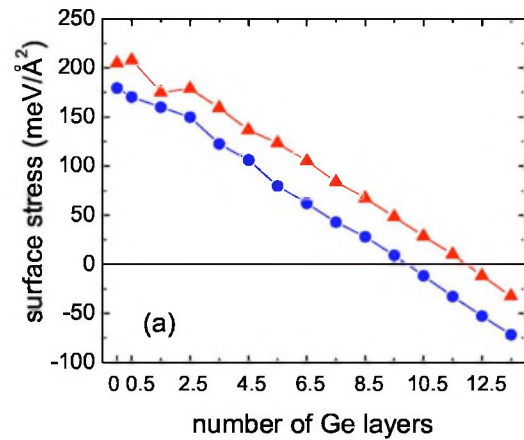


FIG. 3. (Color online) (a) and (b) show surface stresses of the Ge/Si(105) and (001) surfaces, respectively, as a function of the Ge coverage. Circles and triangles represent, respectively, the surface stress in the [010] and $[\bar{5}01]$ direction for the Ge/Si(105) surface, and in the [110] (dimer bond) and $[\bar{1}10]$ (dimer row) direction for the Ge/Si(001) surface. (c) shows the average surface stresses of Ge/Si(105) (circles) and Ge/Si(001) (triangles) surfaces as a function of Ge coverage. The x-axis labels are the same as in Fig. 2. Dashed lines are linear fits to the three high-coverage data points for yielding the Young's modulus.

$103.5 \text{ meV}/\text{\AA}^2$ of the bulk-terminated surface to $94.2 \text{ meV}/\text{\AA}^2$ of the reconstructed surface by eliminating number of dangling bonds in the surface (from 20 to 8) but at

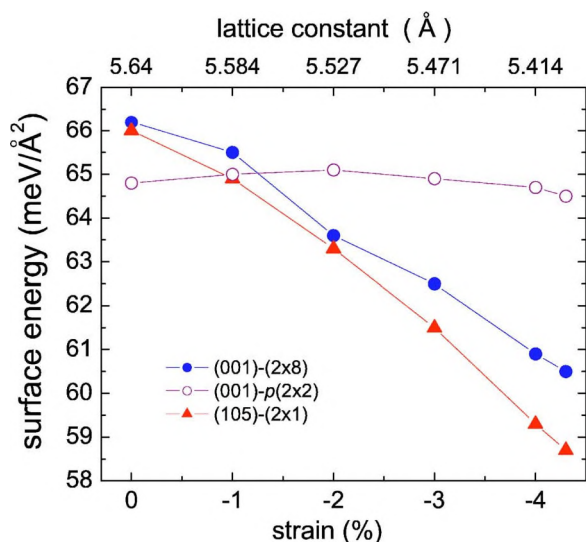


FIG. 4. (Color online) Surface energies of the pure Ge surfaces as a function of strain. Filled circles, open circles, and filled triangles represent the Ge(001)-(2 \times 8), - p (2 \times 2), and Ge(105)-(2 \times 1) surface, respectively.

the expense of the strain energy increase, introducing a large tensile surface stress. For comparison, a large surface stress is also presented on the unstrained Ge(105)-(2 \times 1)-RS surface which is +140.2 and +169.6 meV/Å² in the [010] and $[\bar{5}01]$ directions, respectively. However, they are smaller than those of the Si(105)-(2 \times 1)-RS surface. This again indicates that the (2 \times 1)-RS reconstruction induces a large tensile stress in the surface, but it is partially relieved by the larger Ge atoms in the Ge(105) surface.

Deposition of Ge on Si(105) will retain the same (2 \times 1)-RS reconstruction¹⁴ and, hence, keep the same number of dangling bonds, but at the same time it will relieve the larger tensile stress in the Si(105) surface. Because Ge atoms are \sim 4% larger than Si atoms, the Ge film is under compression, which applies a compressive stress to the surface. Consequently, deposition of Ge will continuously drive the surface towards compression. Figure 3(a) shows Ge deposition reduces the surface stress of Si(105) surface. Thus, it becomes clear that the strained Ge(105) surface is stabilized by the relief of tensile stress in the (2 \times 1)-RS reconstructed surface.

Our calculations show that the Ge-covered Si(105) surface remain tensile until \sim 11 layers of Ge coverage, beyond which the surface will experience a compressive stress increasing linearly with the increase of Ge coverage [Fig. 3(a)]. It indicates that the Ge film deposited on the Si(105) surface is possibly stable up to 11 layers. This agrees quantitatively with the experimental observation that the growth of Ge film on the Si(105) surface continues to proceed via a layer-by-layer growth mode without roughening (or islanding) up to ten layers of Ge deposition.¹⁴

Deposition of Ge drives both the Ge/Si(001) and (105) surfaces toward compression continuously, as shown in Fig. 3. Roughly speaking, the surface stress applied by the Ge film equals its compressive bulk stress times the film thickness. In particular, for a sufficiently thick Ge film when the

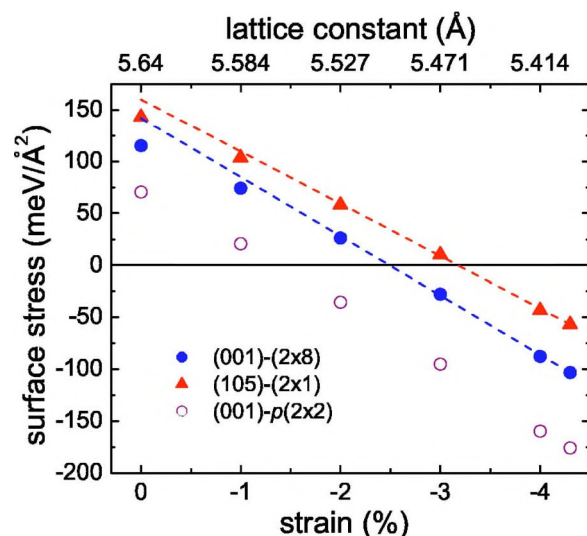


FIG. 5. (Color online) Average surface stresses of the pure Ge surfaces as a function of strain. The notations are the same as in Fig. 4. The dashed lines are linear fits to four high-strain data points of the Ge(001)-(2 \times 8) and Ge(105)-(2 \times 1) surfaces.

reconstructed surface structure remains unchanged (without considering Ge-Si intermixing), the compressive stress applied by the Ge film increases linearly with increasing Ge coverage, with a slope proportional to the Young's modulus of the Ge film and misfit strain. This linear relationship is shown in Fig. 3(c) for both (001) and (105) surfaces. Linear fits to the three high-coverage stress data points yield the Young's moduli 142.7 and 130.7 GPa, respectively. The Young's modulus of 142.7 GPa at the $\langle 110 \rangle$ direction are in good agreement with 138.0 GPa determined by the elasticity theory in the same direction.²¹

In addition, our calculation also confirms the Ge-induced sign reversal of surface stress anisotropy on Si(001) surface [Fig. 3(b)], as observed in the experiment²² and explained by theory.^{4,12}

Using the calculated surface energy and surface stress as input parameters, we have performed quantitative continuum modeling to estimate the critical size for hut nucleation or formation [\sim 110–160 Å (base)], which is in good agreement with the experiments. We also evaluated the magnitude of the surface stress discontinuity at the island edge and the island edge relaxation energy due to such stress discontinuity, which indicated that the effect of the edge relaxation energy is too small to induce a stable island size against coarsening.¹⁵

B. Surface energies and surface stresses of pure Ge(105) and (001) surfaces

To further understand the strain stabilization of the Ge(105) surface and thus the stability of the Ge hut formation on Si(001), we also calculate the surface energies and the surface stresses of pure Ge(105) and (001) surfaces as a function of strain, as shown in Figs. 4 and 5. The p (2 \times 2) and (2 \times 8) reconstructions have been considered for the Ge(001) surface. Because surface stress depends on the film

thickness under external strain, we use approximately the same film thickness ($\sim 22 \text{ \AA}$) for all three cases, corresponding to ten (001)-layers or 25 (105)-layers.

The clean Ge(105) surface has a higher surface energy than the Ge(001)- $p(2 \times 2)$ surface (Fig. 4), which agrees with a recent first-principles calculation.²³ A large tensile surface stress ($+143.3 \text{ meV/\AA}^2$) is presented on the Ge(105) surface due to the (2×1) -RS reconstruction, which is much larger than that of the Ge(001)- $p(2 \times 2)$ surface ($+70.6 \text{ meV/\AA}^2$) (Fig. 5). The instability of the Ge(105) surface arises from its large tensile surface stress, similar to the Si(105) surface.

With increasing compressive strain, surface energies of both the Ge(105) and Ge(001)- (2×8) surfaces decrease, while the surface energy of the Ge(001)- $p(2 \times 2)$ surface remains approximately unchanged.²³ Under the same strain, the surface stress of the Ge(105) surface is always more tensile than that of the Ge(001) surface due mainly to its initially larger tensile surface stress, which agrees with those of the Ge-covered Si surfaces [Fig. 3(c)].

Compressing the Ge(105) surface to the Si lattice constant further lower the surface energy by $\sim 7 \text{ meV/\AA}^2$ than the unstained Ge(105) surface (Fig. 4), indicating the high stability of the Ge(105) surface under compressively strained conditions. Surface stress results (Fig. 5) indicate that strain stabilization of the Ge(105) surface is caused by the reduction of the large tensile stress existing in the unstained Ge(105) surface, which decreases from $+143.3$ to -56.8 meV/\AA^2 in a 25-layer strained Ge film. This again confirms that Si(105) and Ge(105) surfaces are unstable at their respective equilibrium lattice constant, but can be stabilized by the compressive strain through relaxation of the large tensile surface stress originally existing on the Si(105) or Ge(105) surface due to (2×1) -RS reconstruction.

At the strain of 4.3%, the converged surface energy of pure Ge (105) surface is 58.7 meV/\AA^2 , only a slight different from that of the Ge-covered Si surface ($\sim 61.4 \text{ meV/\AA}^2$). The difference between the surface energies of pure Ge(001) and Ge-covered Si(001) surface is much smaller. Considering that the calculated surface energies of the Ge-covered Si surface include Ge-Si interfacial energy, while those of the pure Ge surface do not, the results thus imply a small interfacial energy between Si and Ge.

In addition, the strain-dependence of the surface energy of the pure Ge surfaces also demonstrates the reconstruction transformation from Ge(001)- $p(2 \times 2)$ to $-(2 \times 8)$ with increasing compressive strain. Initially the Ge(001)- $p(2 \times 2)$

surface has a lower surface energy than Ge(001)- (2×8) , and thus the unstrained Ge(001) surface exhibits $p(2 \times 2)$ reconstruction. They become equal between the compressive strain of 1% and 2%, beyond which the surface energy of the Ge(001)- (2×8) surface becomes lower, indicating that the (2×8) reconstruction becomes more stable under larger compression. Under the compressive strain of 4.3%, the surface energy of the Ge(001)- (2×8) surface is 60.5 meV/\AA^2 , $\sim 4 \text{ meV/\AA}^2$ lower than that of $-p(2 \times 2)$ surface. Therefore, the Ge-covered Si(001) surface exhibits $(2 \times N)$ reconstruction.

Finally, we determine the Young's modulus by fitting the surface stress versus the strain curve in Fig. 5. The calculated Ge Young's moduli are, respectively, 143.2 GPa for the (001) Ge film and 125.6 GPa for the (105) Ge film, in good agreement with those obtained by fitting the surface stress versus the Ge coverage in the Ge/Si() film (Fig. 3) and with the elasticity theory.²¹

IV. SUMMARY

In summary, we have calculated the surface energies, surface stresses, and their strain dependence of the Ge/Si(001) and (105) surfaces as a function of the Ge coverage, using the first-principles total-energy method. We show that originally the surface energy of the Si(105) surface is higher than that of Si(001), but it can be reduced by the Ge deposition, making it almost degenerate with that of the Ge-covered Si(001) surface at about the wetting layer thickness, which leads to the $\{105\}$ -faceted Ge hut formation. We demonstrate that, unlike the stable Si(001) surface, the original unstrained Si(105) and Ge(105) surfaces are unstable because a large tensile stress present in both surfaces due to surface reconstruction to eliminate dangling bonds, but they can be largely stabilized by applying an external compressive strain, such as by deposition of the Ge layers on the Si(105) surface. Our study quantitatively reveals that the strain stabilization of the Ge(105) facets is the physical origin of the Ge hut formation.

ACKNOWLEDGMENTS

This work is supported by the U.S. Department of Energy (DE-FG03-01ER45875; DE-FG-03ER46027). G.-H.L. is grateful for support from the National Natural Science Foundation of China (NSFC) and Dr. Fujikawa for helpful discussion. The calculations were performed on IBM SP RS/6000 at NERSC and ORNL, and AMD Opteron cluster at the CHPC, University of Utah.

*Electronic address: fliu@eng.utah.edu

¹E. Bauer, Z. Kristallogr. **110**, 372 (1958).

²D. J. Eaglesham and M. Cerullo, Phys. Rev. Lett. **64**, 1943 (1990).

³Y.-W. Mo, D. E. Savage, B. S. Swartzentruber, and M. G. Lagally, Phys. Rev. Lett. **65**, 1020 (1990).

⁴F. Liu, F. Wu, and M. Lagally, Chem. Rev. (Washington, D.C.)

97, 1045 (1997).

⁵F. Liu and M. Lagally, Surf. Sci. **386**, 169 (1997).

⁶V. Shchukin and D. Bimberg, Rev. Mod. Phys. **71**, 1125 (1999).

⁷J. Stangl, V. Holy, and G. Bauer, Rev. Mod. Phys. **76**, 725 (2004).

⁸Y. Fujikawa, K. Akiyama, T. Nagao, T. Sakurai, M. G. Lagally, T. Hashimoto, Y. Morikawa, and K. Terakura, Phys. Rev. Lett. **88**,

- 176101 (2002).
- ⁹T. Hashimoto, Y. Morikawa, Y. Fujikawa, T. Sakurai, M. Lagally, and K. Terakura, *Surf. Sci.* **513**, L445 (2002).
- ¹⁰P. Raiteri, D. B. Migas, L. Miglio, A. Rastelli, and H. von Kanel, *Phys. Rev. Lett.* **88**, 256103 (2002).
- ¹¹K. Khor and S. das Sarma, *J. Vac. Sci. Technol. A* **15**, 1051 (1995).
- ¹²F. Liu and M. G. Lagally, *Phys. Rev. Lett.* **76**, 3156 (1996).
- ¹³K. Varga, L. Wang, S. Pantelides, and Z. Zhang, *Surf. Sci.* **562**, L225 (2004).
- ¹⁴M. Tomitori, K. Watanabe, M. Kobayashi, F. Iwawaki, and O. Nishikawa, *Surf. Sci.* **301**, 214 (1994).
- ¹⁵G.-H. Lu and F. Liu, *Phys. Rev. Lett.* **94**, 176103 (2005).
- ¹⁶G. Kresse and J. Hafner, *Phys. Rev. B* **47**, R558 (1993).
- ¹⁷G. Kresse and J. Furthmüller, *Phys. Rev. B* **54**, 11169 (1996).
- ¹⁸G.-H. Lu, M. Huang, M. Cuma, and F. Liu, *Surf. Sci.* **588**, 61 (2005).
- ¹⁹D. Vanderbilt, *Phys. Rev. Lett.* **59**, 1456 (1987).
- ²⁰U. Köhler, O. Jusko, B. Müller, M. H. von Hoegen, and M. Pook, *Ultramicroscopy* **42-44**, 832 (1992).
- ²¹W. Brantley, *J. Appl. Phys.* **44**, 534 (1973).
- ²²F. Wu and M. G. Lagally, *Phys. Rev. Lett.* **75**, 2534 (1995).
- ²³D. Migas, S. Cereda, F. Montalenti, and L. Miglio, *Surf. Sci.* **556**, 121 (2004).